

Recent Results from CANGAROO

MASAKI MORI* for the CANGAROO team

*Institute for Cosmic Ray Research, University of Tokyo,
Kashiwa, 277-8582 Chiba, Japan*

**E-mail: morim@icrr.u-tokyo.ac.jp
http://icrhp9.icrr.u-tokyo.ac.jp/*

The CANGAROO-III telescope system for very-high-energy gamma-ray astrophysics consists of four 10-m atmospheric Cherenkov telescopes located near Woomera, South Australia. The construction of the fourth telescope was completed in summer 2003, and stereoscopic observations have been in progress since March 2004. Here we report on the status of the system and some recent results from CANGAROO-III observations.

Keywords: gamma rays; observation; atmospheric Cherenkov telescopes

1. Introduction

CANGAROO is an acronym for the Collaboration of Australia and Nippon (Japan) for a GAMMA Ray Observatory in the Outback. After successful operation of the 3.8m imaging Cherenkov telescope (CANGAROO-I) for 7 years, which was the first of this kind in the southern hemisphere, we constructed a new telescope of 7m diameter (CANGAROO-II) in 1999 next to the 3.8m telescope near Woomera, South Australia ($136^{\circ}47'E$, $31^{\circ}06'E$, 160m a.s.l.). Then the construction of an array of four 10m telescopes (CANGAROO-III) was approved and as the first step the 7m telescope was upgraded to 10m diameter in 2000, with this becoming the first telescope of the CANGAROO-III array (T1).¹ Results from observations with this first 10m telescope have been reported in publications (see, e.g.¹).

In the following years, we have constructed an additional three 10m telescopes located at the corners of a diamond of 100m sides with improved mirrors, cameras and electronics. After tuning, we have started observation with the full system in stereo mode in March 2004. Here we report recent results from stereo observations with CANGAROO-III.

2. Stereo analysis: the case of the Crab nebula

The Crab nebula is the first established TeV gamma-ray source and is used as a calibration source to check performance of a Cherenkov telescope. However, from Woomera, it can be observed only at large zenith angles ($> 53^\circ$). For stereo observations, the threshold energy of T1 is higher than other telescopes and thus we used the newer three telescopes (T2, T3 and T4 in the order of construction) for analysis. Because of the geometrical arrangement of the array, the effective baseline for large zenith angle observations becomes short which makes stereo reconstruction of images difficult.

To overcome the unfortunate situation described above, we developed new analysis methods.² To avoid the increased uncertainty of the intersection points, we introduced a new parameter, “IP distance” (D_{IP}), which is defined as the distance between the intersection point and centroid of images. Then we searched for the intersection point which minimized the image widths and the difference between distance and D_{IP} . This results in better angular resolution as seen in the θ^2 distribution in Monte Carlo simulations, where θ is the space angle between the source direction and the reconstructed arrival direction: gamma-ray signals should be seen as a peak toward $\theta^2 = 0$, whose sharpness depends on the angular resolution and the angular extent of a gamma-ray source.

We observed the Crab nebula in December 2003 in so-called “wobble” mode, changing the pointing directions $\pm 0.5^\circ$ in declination from the target every 20 minutes, with a two-fold stereo mode (T2 and T3: T4 was not completed at that time). After basic data quality check, such as rejecting runs affected by clouds, a total of 890 minutes data were used for further analysis.

In addition to the conventional square cuts method using image parameters to enhance gamma-ray fractions, we applied two different analyses: the Likelihood method^{3,4} and the Fisher Discriminant method.^{2,5} In the latter method, effectiveness of the parameters for the gamma-ray-like event selection is evaluated using the simulation, and we can optimize the weights of the imaging parameters (*width* and *length* in this case) automatically by matrix inversion in estimating the probability of gamma-ray-like events, eliminating ambiguities in parameter cut positions. Finally we obtained the spectrum of the Crab nebula in the energy range from 2 to 20 TeV,⁵ which is consistent within the statistical and systematic errors with other measurements.^{6,7}

3. Recent results

3.1. Pulsar PSR 1706-44

A detection of a gamma-ray signal from PSR 1706-44, which was one of the EGRET-detected pulsars, was reported using the data acquired by CANGAROO-I 3.8m telescope.⁸ The Durham group also reported a detection with their Mark 6 telescope.⁹ H.E.S.S., however, claimed no detection from that direction.¹⁰ We observed this source for 27 hours (ON) and 29 hours (OFF) with CANGAROO-III in May 2004. Preliminary analyses using T2 and T3 telescope pair did not show a peak in the θ^2 distribution.¹¹ The upper limit from this result is shown in Fig. 1, which is lower than the flux reported by CANGAROO-I. Further analysis is underway and the details will be reported elsewhere.

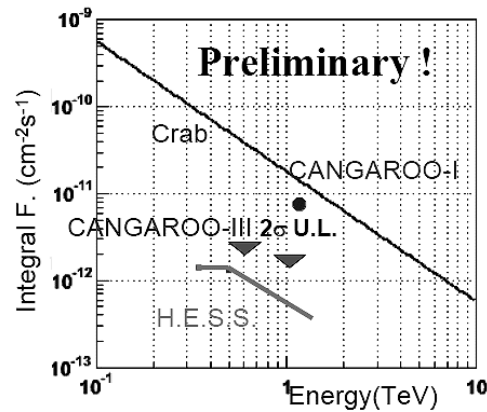


Fig. 1. Upper limits on gamma-ray flux from PSR 1706-44 from CANGAROO-III observations (triangle).¹¹ The CANGAROO-I result is shown by a filled circle⁸ and the H.E.S.S. limits¹⁰ are also shown.

3.2. Supernova remnant SN1006

A detection of a gamma-ray signal from SN1006, which was shown to be a source of high-energy electrons through observation of non-thermal X-rays with ASCA,¹² was reported using the data acquired by CANGAROO-I.¹³ H.E.S.S., however, claimed no detection from that direction.¹⁴ We observed this source for 27 hours (ON) and 29 hours (OFF) with CANGAROO-III in May 2004. Preliminary analyses using T2 and T3 telescope pair did not show any peaks in the θ^2 distribution for the NE-rim point which

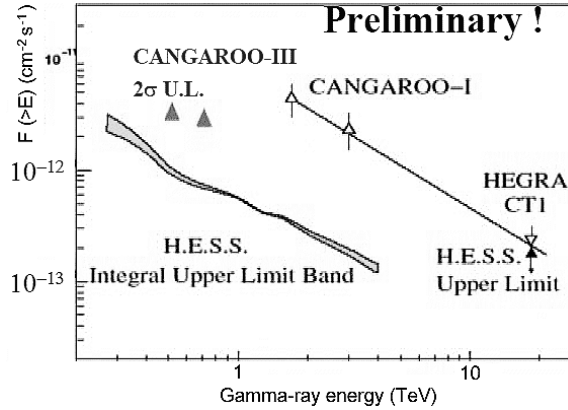


Fig. 2. Upper limits on gamma-ray flux from NE-rim of SN1006. The CANGAROO-I results are shown by open triangles¹³ and the HEGRA CT1 result by inverted open triangle.¹⁵ The CANGAROO-III upper limits¹¹ are shown by filled triangles with H.E.S.S. limits.¹⁹

was the maximum point of the gamma-ray emission in the CANGAROO-I data.¹³ The upper limit from this result is lower than the flux reported by CANGAROO-I. Further analysis is underway to check for possible extended emission, and the details will be reported elsewhere.

3.3. Vela pulsar and nebula

The Vela pulsar was observed in January/February 2004. After basic data quality check, a total of 1311 minutes data were used for further analysis,⁵ where the minimum elevation angle was set at 60° . The mean elevation angle was 70.9° , corresponding to an energy threshold of 600 GeV. The observations were carried out using the same wobble mode as for the Crab nebula observations. In this period, T2 and T3 were in operation, and we analyzed the stereo data from these two telescopes. For Vela, at a declination of -45° , the relative orientation of the two telescopes does not present any problems.

We used the optimized analysis procedure used for the Crab nebula analysis described above. The resulting θ^2 distribution for the Vela pulsar position showed no significant gamma-ray signal, giving upper limits as shown in Fig.3, which are consistent with H.E.S.S. results.¹⁹ Also we did not see excess from the point offset by 0.13° from the pulsar, which was the maximum of the excess detected with the CANGAROO-I telescope.¹⁶

The H.E.S.S. group detected a gamma-ray excess from the Vela X neb-

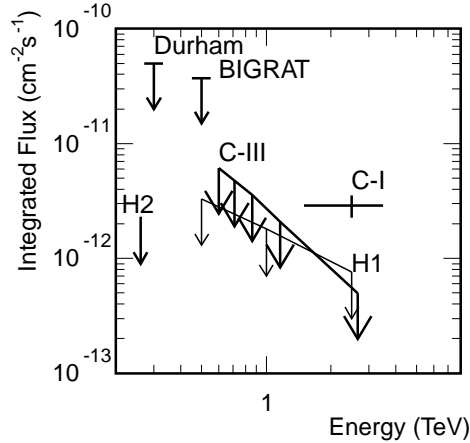


Fig. 3. The 2σ upper limits for the gamma-ray flux from the Vela pulsar by CANGAROO-III (C-III).⁵ C-I represents the CANGAROO-I excess from the point offset by 0.13° from the pulsar.¹⁶ Also shown are upper limits reported by the Durham group,¹⁷ BIGRAT¹⁸ and H.E.S.S..¹⁹

ula, extended over a 0.6° radius from the center of the emission [(R.A., decl.) = ($8^{\text{h}}35^{\text{m}}$, $-45^\circ36'$), J2000].¹⁹ In order to analyze extended emission, we applied the following method. Gamma-ray-like events can be extracted by fitting position-by-position F (Fischer discriminant) distributions under the assumption that gamma rays obey the Monte Carlo predictions, the proton background follows the average F distribution of all directions, and the total distribution is a linear combination of those two. We chose the background region to be more than 0.8° from the center, since we do not have sufficient statistics for off-source regions for these observations. The result of fitting is shown in Fig. 4. An excess was observed at $\theta^2 < 0.6 \text{ deg}^2$ around the center of the Vela X region. The excess radius is marginally consistent with H.E.S.S. considering our angular resolution. The total number of gamma-ray-like events is 561 ± 114 . Though the statistical significance is below the 5σ level, this could be supporting evidence of the H.E.S.S. detection. The differential fluxes for the excess regions are in general agreement with H.E.S.S. result.⁵

3.4. SNR RX J0852.0-4622

We already reported a gamma-ray signal from this SNR using observations by CANGAROO-II in 2001 and 2002.²⁰ This time we applied the Fisher

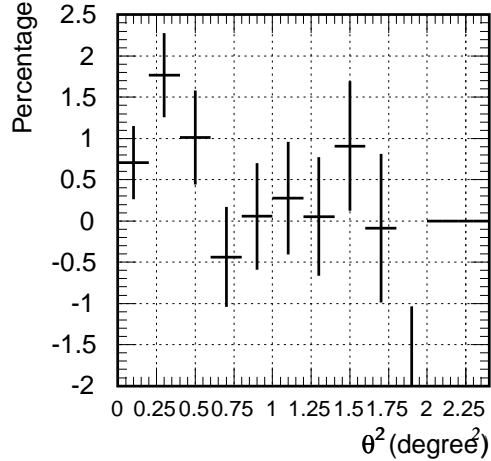


Fig. 4. Wide-range θ^2 plot for the Vela X region,⁵ where θ is a space angle of an event direction from (R.A., decl.) = ($8^{\text{h}}35^{\text{m}}, -45^{\circ}36'$) [J2000], i.e., the peak of the emission detected by H.E.S.S..¹⁹

discriminant method to the stereo data for RX J0852.0-4622 observed in January and February 2005 using T2, T3 and T4 taken in the wobble mode. After the coarse selections, 1,129 minutes (ON) and 1,081 minutes (OFF) data were available. For the Fisher discriminant, we used six image parameters, lengths and widths, determined with each telescope independently. Finally the gamma-ray events were extracted by comparing the Fisher discriminant values between the SNR region and the background region. The excess count map is shown in Figure 5.²² The smoothing was carried out using the average of the center and neighboring eight pixels where the pixel size was $0.2^{\circ} \times 0.2^{\circ}$. The dotted circle of 1 degree from the supernova center is also shown. The strong gamma-ray emission from the NW rim is obviously seen, which was first reported by CANGAROO-II.²⁰ The emission profile shows shell-like structure like that seen in X-rays. The differential energy spectra for the whole remnant are shown in Figure 6. The agreement of the CANGAROO-III result with that of H.E.S.S.²¹ is reasonable. The energy spectrum around the NW-rim was measured to be consistent with that of the whole remnant, i.e., flatter than that reported from the previous CANGAROO-II data. The difference can be partially explained by the deterioration of the hardware of the CANGAROO-II telescope.

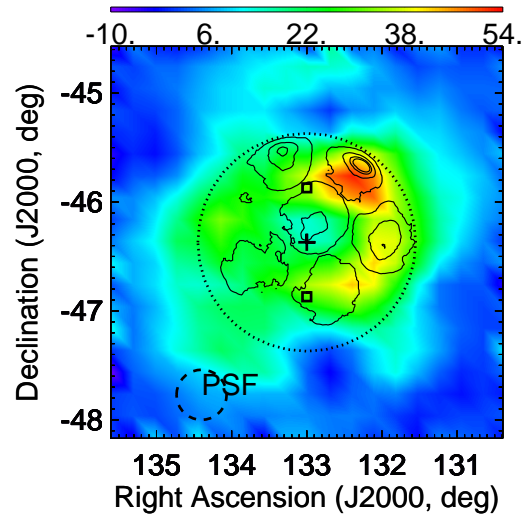


Fig. 5. Excess event map around the SNR RX J0852.0-4622 obtained from the CANGAROO-III stereo observations in 2005.²² The vertical scale (number of events per pixel, $0.2^\circ \times 0.2^\circ$) is indicated in the top bar. The cross indicates the average pointing position, i.e., the center of the remnant and the squares the “wobble” pointing positions. The dashed circle of 0.23° shows the (1σ) point spread function. Overlaid contours show X-ray intensity observed by ASCA GIS.

4. Summary

We have been carrying out stereo observations of sub-TeV gamma-rays with CANGAROO-III since March 2004. Results from stereo observations were presented: PSR 1706-44 and SN1006, from which gamma-ray signals were reported by CANGAROO-I, were not confirmed by CANGAROO-III observations. For two supernova remnants, the Vela SNR and RX J0852.0-4622, our results are consistent with the recent H.E.S.S. results.

The distribution of ‘gamma-ray SNRs’ is important in the quest for the origin of cosmic-rays and the high-energy content of the Universe: we will continue systematic study of SNRs in high-energy gamma-rays in the Galaxy.

References

1. Masaki Mori, *Science with the New Generation of High Energy Gamma-ray Experiments*, eds. A. De Angelis and O. Mansutti (World Scientific, Singapore, 2006), pp.21-28 and references therein.

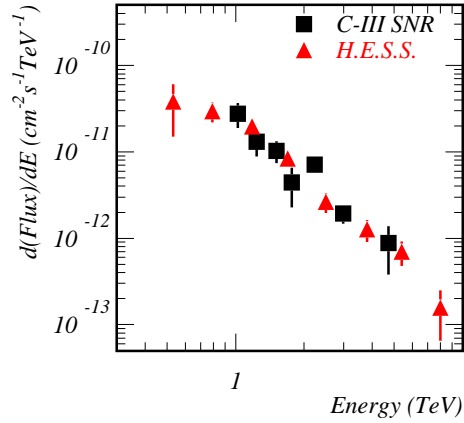


Fig. 6. Differential energy spectra; squares are data points obtained by CANGAROO-III observation for the whole remnant,²² and triangles are by H.E.S.S..²¹ The error bars are statistical.

2. T. Nakamori et al., in *Proc. 29th ICRC (Pune)* (Tata Inst. Fundamental Research, India, 2005), Vol. 4, pp. 203–206.
3. R. Enomoto et al., in *Proc. 27th ICRC (Hamburg)* (Copernicus Gesellschaft, Germany, 2001), Vol.5, pp. 2477–2480.
4. R. Enomoto et al., *Nature* **416**, 823–826 (2002).
5. R. Enomoto et al., *Astrophys. J.* **638**, 397–408 (2006).
6. F.A. Aharonian et al., *Astrophys. J.* **539**, 317–324 (2000).
7. A.M. Hillas et al., *Astrophys. J.* **503**, 744–759 (1998).
8. T. Kifune et al., *Astrophys. J.* **438**, L91–94 (1995).
9. P.M. Chadwick et al., *Astropart. Phys.* **9**, 131–136 (1998).
10. F.A. Aharonian et al., *Astron. Astrophys.* **432**, L9–L12 (2005).
11. T. Tanimori et al., in *Proc. 29th ICRC (Pune)* (Tata Inst. Fundamental Research, India, 2005), Vol. 4, pp. 215–218.
12. K. Koyama et al., *Nature*, **278**, 255–228 (1995).
13. T. Tanimori et al., *Astrophys. J.* **497**, L25–28 (1998).
14. F.A. Aharonian et al., *Astron. Astrophys.* **437**, 135–139 (2005).
15. V. Vitale et al., in *Proc. 28th ICRC (Tsukuba)* (Universal Academy Press, Tokyo, 2003), pp. 2889–2892.
16. T. Yoshikoshi et al., *Astrophys. J.* **487**, L65–68 (1997).
17. P.M. Chadwick et al., *Astrophys. J.* **537**, 414–421 (2000).
18. S.A. Dazeley, Ph.D. thesis, University of Adelaide (1999).
19. F.A. Aharonian et al., *Astron. Astrophys.* **448**, L43–47 (2006).
20. H. Katagiri et al., *Astrophys. J.* **619**, L163–L165 (2005).
21. F. Aharonian et al., *Astron. Astrophys.* **437**, L7–10 (2005).
22. R. Enomoto et al., *Astrophys. J.*, **653**, in press (2006).